PCCP

PAPER

View Article Online
View Journal | View Issue

Cite this: *Phys. Chem. Chem. Phys.*, 2018, **20**, 6299

Ternary CBe_4Au_4 cluster: a 16-electron system with quasi-planar tetracoordinate carbon†

Jin-Chang Guo,‡[ab] Lin-Yan Feng‡[b] and Hua-Jin Zhai *[b]

Received 16th December 2017,
Accepted 29th January 2018

DOI: 10.1039/c7cp08420j

rsc.li/pccp

Planar hypercoordinate carbons as exotic chemical species are dominated by 18-electron counting. We report herein a 16-electron planar tetracoordinate carbon (ptC) cluster, CBe_4Au_4, which is quasi-planar to be exact, being composed of a C center, a square-planar Be_4 ring, and four outer Au bridges. The quasi-ptC cluster is established as a global minimum *via* computer structural searches, located 14.6 kcal mol^{-1} below the nearest competitor at the CCSD(T) level. It shows thermodynamic and electronic robustness, with a low electron affinity (1.54 eV at B3LYP) and a large HOMO–LUMO gap (2.21 eV for excitation energy). Bonding analyses reveal 2π and 6σ double aromaticity, in addition to four three-center two-electron (3c-2e) Be–Au–Be σ bonds, confirming that 16-electron counting is perfect for the system. We believe that double (π and σ) aromaticity is a general concept that governs planar or quasi-planar carbons, which overrides the 18-electron rule. Competition between quasi-ptC and tetrahedral carbon (thC) isomers in the CBe_4M_4 (M = K, Au, H, Cl) series is also examined, which sheds crucial light on factors that govern the ptC clusters. The present findings offer opportunities for further planar and unconventional molecules.

1. Introduction

Planar hypercoordinate carbon molecules[1–22] have been researched for half a century since the introduction of the idea of planar tetracoordinate carbon (ptC) by Monkhorst in 1968,[3] who hypothesized that the transition state in interconversion of enantiomers containing asymmetric carbon atoms can involve a ptC, albeit without trying to stabilize such species. These studies are motivated by pure chemical curiosity to understand, alter, and design unconventional chemical bonds surrounding a carbon center. As a consequence, planar hypercoordinate carbons are normally quite unstable with respect to their tetrahedral carbon (thC) rivals. Only a handful of them are thermodynamically stable and viable, despite 50 years of pursuit in the field.[1] Notable examples of planar hypercoordinate carbons are (i) 1,1-dilithiocyclopropane, the first stable ptC molecule (relative to thC) as predicted by Pople and co-workers;[5] (ii) the observation *via* photoelectron spectroscopy (PES) of a series of CAl_4^{2-} based ptC clusters ($NaCAl_4^-$, CAl_3Si^-, and CAl_3Ge^-)[6–10] by Wang and Boldyrev, which are isovalent to the *cis*-CAl_2Si_2 and *trans*-CAl_2Si_2 species computed earlier by Schleyer, Boldyrev, and Simons;[6,7] (iii) the discovery of the D_{5h} CAl_5^+ cluster as global minimum (GM) by Zeng and co-workers,[11] which contains planar pentacoordinate carbon (ppC); and (iv) computer design of "hyparenes" by Schleyer[12] including a planar hexacoordinate carbon (phC) CB_6^{2-} cluster, the latter being unfortunately a highly energetic local-minimum (LM) only.

In key literature on ptC and ppC clusters, the 18-electron counting appears to be predominant. This was initiated by Schleyer and Boldyrev in their 1991 ptC paper, which stated that eighteen electrons are necessary and are the magic number for planar species of this type.[6] Boldyrev and Simons[7] subsequently reiterated the importance of 18-electron counting for ptC, as well as three C-ligand σ bonds and one C-ligand π bond, although the term "aromaticity" was not used. Indeed, CAl_4^{2-} or CAl_5^+ based clusters represent extensive and expanding classes of ptC/ppC complexes,[6–11,14–22] which are all 18-electron systems. Many of the species were deliberately designed by following this magic counting, stated or not. For example, the $NaCAl_4^-$ monoanion cluster was experimentally produced as a salt complex, $Na^+[CAl_4^{2-}]$, so that ptC CAl_4^{2-} unit is maintained with exactly

[a] *Department of Chemistry, Xinzhou Teachers University, Xinzhou 034000, Shanxi, China*
[b] *Nanocluster Laboratory, Institute of Molecular Science, Shanxi University, Taiyuan 030006, China. E-mail: hj.zhai@sxu.edu.cn*

† Electronic supplementary information (ESI) available: Orbital composition analyses for global-minimum **1** of CBe_4Au_4 clusters, as well as those of C_{4v} and T_d isomers of CBe_4M_4 (M = K/Au/H/Cl) (Tables S1–S3); optimized ptC or quasi-ptC clusters **1–3** of $CBe_4Au_4^{0/-/2-}$ and three lowest-lying isomers (***n*B–*n*D**) at B3LYP/def2-TZVP (Fig. S1); Wiberg bond indices (WBIs) for **1–3** (Fig. S2); selected optimized salt complexes based on dianion $CBe_4Au_4^{2-}$ (**3**) cluster at B3LYP (Fig. S3); WBIs for structures **4–8** of $CAl_4^{0/-/2-}$ (Fig. S4); optimized quasi-ptC C_{4v} structures **9–11** of CBe_4M_4 (M = K/H/Cl) and their T_d counterparts (Fig. S5); WBIs for selected structures of CBe_4M_4 (M = K/H/Cl) and CAl_4 (Fig. S6); calculated NICSs for **1–3** (Fig. S7); and CMOs of structures **4** and **5** of CAl_4 (Fig. S8). See DOI: 10.1039/c7cp08420j

‡ These authors contributed equally to this work.

18 electrons.[9] Similarly, Bowen and co-workers[21] conducted an experimental study on the ptC CAl_4H^- cluster, in which the H atom serves to test and manifest the 18-electron rule, as stated. Merino and co-workers computationally designed a series of CBe_5^{4-} based derivatives and extended the 18-electron preference rule, as explicitly stated, from ptCs to ppCs.[17]

Thus it seems to be fair to say that in the literature this magic electron-counting is a "rule" for such exotic species. In fact, this is the very reason why dianions, tetraanions, cations, and salt complexes were computationally designed or experimentally characterized. However, it remains unclear why 18-electron counting is needed for a two-dimensional (2D) or quasi-2D cluster. One may argue that 2D species follow distinct electron-counting rules as compared to typical 3D systems, on which the 18-electron rule is based. A 2D free-electron nanosystem, for instance, has revised magic numbers with 6-, 8-, and 12-electrons, and so on, in which 18-electron is nonexistent.[23] This is in sharp contrast to the 3D shell model.[24]

Is 18-electron counting really required in order to stabilize the ptC/ppC complexes? Is it merely coincidental? Can other electron-counting be electronically better suited for specific ptC systems? Indeed, the electron counting rule for ptCs is known to depend strongly on the chemical surrounding, which can be found in particular in the excellent review by Keese.[2] Herein we seek to address these questions using a ternary C–Be–Au system. Specifically, we explore $CBe_4Au_4^{0/-/2-}$ clusters with 16, 17, and 18 electrons, which are isovalent to the $CAl_4^{0/-/2-}$ species.[6–10] While 18-electron CAl_4^{2-} based species (and 17-electron CAl_4^-) are ptC complexes, 16-electron neutral CAl_4 is known to be a thC cluster.[8] The lowest planar isomer of neutral CAl_4 contains a tricoordinate carbon, rather than ptC. In this work, our computer global structural searches show that $CBe_4Au_4^{0/-/2-}$ (**1–3**) clusters all assume star-like structures with ptC or quasi-ptC. In particular, C_{4v} CBe_4Au_4 (**1**) as a quasi-planar cluster is rather well defined on its potential energy surface, being 14.60 kcal mol^{-1} more stable than the nearest isomer at the CCSD(T) level, which differs distinctly from the isovalent, thC CAl_4 cluster. To our knowledge, the CBe_4Au_4 (**1**) cluster is the first example of ptC (or quasi-ptC) with 16-electron counting.

Chemical bonding analyses suggest that the quasi-ptC CBe_4Au_4 (**1**) cluster possesses 2π and 6σ double aromaticity, in addition to four Be–Au–Be three-center two-electron (3c-2e) σ bonds on the periphery, thus forming an ideal electronic system without the need to fulfill the so-called 18-electron rule. We believe that the presence of one π and three σ delocalized bonds in planar hypercoordinate carbons (or more generally, π/σ double aromaticity) is necessary to stabilize such systems, even without fulfilling the 18-electron counting. The latter is not a law; it is only a guide. This understanding suggests further opportunities to design planar, unconventional molecules.

2. Methods

Structural searches were performed for neutral CBe_4Au_4 and its $CBe_4Au_4^{2-}$ dianion, using the Coalescence Kick (CK) algorithm[25–27] at the hybrid B3LYP/lanl2dz level.[28,29] More than 1000 stationary points were probed on the potential energy surface for each of the species, primarily focusing on singlets. About 800 triplet structures were also searched for neutral CBe_4Au_4. Top low-lying isomers were subsequently re-optimized at the B3LYP/def2-TZVP level.[30] Low-lying isomers of the $CBe_4Au_4^-$ monoanion were obtained on the basis of those of the neutral and dianion species, and no independent CK searches were performed for $CBe_4Au_4^-$. Frequency calculations were done at B3LYP/def2-TZVP to ensure that the reported structures are true minima, unless stated otherwise. To benchmark the energetics, single-point CCSD(T) calculations[31–33] were carried out for top four isomers at the B3LYP/def2-TZVP geometries.

Natural bond orbital (NBO) analyses[34] were carried out at B3LYP/def2-TZVP to obtain natural atomic charges and Wiberg bond indices (WBIs). Nucleus independent chemical shifts (NICSs)[35] were calculated to assess π/σ aromaticity for selected species. Vertical detachment energies (VDEs) and electron affinities (EAs) were calculated using the time-dependent B3LYP (TD-B3LYP) method.[36,37] All electronic structure calculations were done using Gaussian 09.[38] Molecular structures and canonical molecular orbitals (CMOs) were visualized using CYLview and GaussView 5.0.[39,40]

3. Results

3.1. Planar tetracoordinate carbon (ptC) $CBe_4Au_4^{0/-/2-}$ clusters

Top low-lying structures of $CBe_4Au_4^{0/-/2-}$ as identified from our CK global searches are shown in Fig. 1 and Fig. S1 (ESI†). Species **1–3** are the GM structures of the neutral, monoanion, and dianion, respectively, which are 14.60, 4.15, and 5.49 kcal mol^{-1}

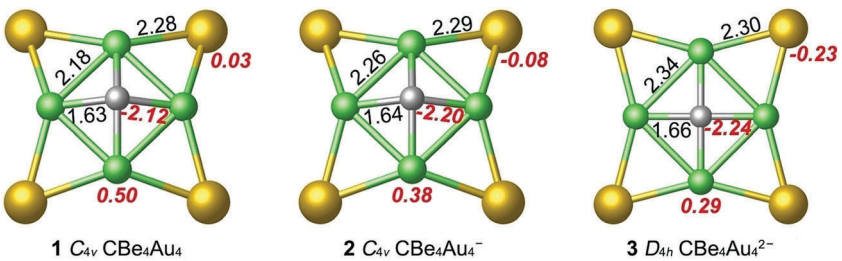

1 C_{4v} CBe_4Au_4 **2** C_{4v} $CBe_4Au_4^-$ **3** D_{4h} $CBe_4Au_4^{2-}$

Fig. 1 Optimized global-minimum (GM) structures at the B3LYP/def2-TZVP level for CBe_4Au_4 (**1**, C_{4v}, $^1A_1$), $CBe_4Au_4^-$ (**2**, C_{4v}, $^2B_1$), and $CBe_4Au_4^{2-}$ (**3**, D_{4h}, $^1A_{1g}$). Bond distances (in Å) and natural atomic charges (in |e|; red color) are shown.

more stable than their closest competitors at the single-point CCSD(T) level. In terms of energetics, GM **1** of neutral $CBeAl_4$ is particularly well defined on its potential energy surface.

Bond distances, NBO charges, and WBIs of **1–3** are presented in Fig. 1 and Fig. S2 (ESI†). For reference, a single C–Be bond has an upper bound of 1.77 Å and that of Au–Be is 2.26 Å, based on the covalent atomic radii.[41] The Be_2 dimer is van der Waals type (2.45 Å)[42] and Be_2^+ with a half bond is 2.21 Å.[43] Thus C–Be bonding in **1–3** (1.63–1.66 Å) is relatively uniform and strong, probably beyond a single bond. The Au–Be bridging bond (2.28–2.30 Å) is also strong, being marginally weaker than the single bond. In contrast, the peripheral Be–Be link expands gradually with charge state (2.18, 2.26, and 2.34 Å from **1** to **3**), the shortest one being close to a half bond. Expansion of the Be–Be link facilitates planarization of ptC or quasi-ptC clusters, with an overall out-of-plane distortion of 0.52 Å for **1**, 0.38 Å for **2**, and none for **3**. GM **3** is perfectly planar. The WBI data are consistent with these analyses (Fig. S2, ESI†). However, the WBI values are markedly lower than the bond orders described above, due to mixed ionic/covalent nature of C–Be and Au–Be bonding, as also reflected from the NBO charges (Fig. 1).

Strictly speaking, the title cluster, 16-electron GM **1** of neutral CBe_4Au_4, is quasi-planar only. However, the out-of-plane distortion in **1** and **2** is about 1/6 to 1/8 with respect to the diagonal Be–Be distance, indicating that these clusters are rather flat and can be approximately called planar. Note that here in this paper, "ptC" is relative to "thC", which are distinct isomers. In this context, ptC and quasi-ptC do not make a fundamental difference. In response to a reviewer, we also note that the dianion ptC $CBe_4Au_4^{2-}$ (**3**) cluster may be stabilized as salt complexes. Selected structures of $CBe_4Au_4Na^-$ and $CBe_4Au_4Na_2$ at the B3LYP/def2-TZVP level are shown in Fig. S3 (ESI†). The structures are true minima on their potential energy surfaces, in which the CBe_4 core is preserved, with slight out-of-plane distortions of 0.38 and 0.39 Å, respectively. Such distortion is smaller than cluster **1** and comparable to **2**. In short, these salt complexes are quasi-ptC species.

Among the low-lying isomers in Fig. S1 (ESI†), six out of nine also contain a quasi-planar CBe_4 core: **1B**, **2B–2D**, **3B**, and **3C**. In all cases, Be_4 in the CBe_4 core does not form a closed ring, primarily due to asymmetric coordination of Au atoms (terminal or bridging). Thus, CBe_4 has great potential to support a ptC or quasi-ptC center, albeit being highly distorted for the majority of the isomers. It appears that an Au bridge brings two Be atoms closer, whereas Au terminal breaks a Be–Be link. Indeed, a 3D isomer with four Au terminals has D_{4h} geometry, perfectly planar and completely open, although it is 26.98 kcal mol^{-1} above GM **3**. Interestingly, the isovalent $CBe_4H_4^{2-}$ dianion[44] was previously shown to have a 3D structure as GM. Therefore, despite the Au/H isolobal analogy,[45–47] $CBe_4Au_4^{2-}$ and $CBe_4H_4^{2-}$ clusters have distinct potential landscapes.

3.2. Typical structures of $CAl_4^{0/-/2-}$ clusters and quasi-ptC *versus* thC isomers of CBe_4M_4 (M = K, H, Cl)

For comparison with $CBe_4Au_4^{0/-/2-}$ (**1–3**), we re-optimized selected structures of their isovalent $CAl_4^{0/-/2-}$ species (Fig. 2).[8,9] The neutral CAl_4 cluster assumes thC GM, **4** (T_d, $^1A_1$), with a tricoordinate carbon LM **5** (C_{2v}, $^1A_1$) being located 9.55 kcal mol^{-1} higher at CCSD(T). The perfect ptC structure **6** (D_{4h}, $^1A_{1g}$) is a third-order saddle point at 15.30 kcal mol^{-1}, which converts to **5** upon removal of imaginary frequencies. The monoanion and dianion are perfect ptC clusters, **7** (D_{4h}, $^2B_{2g}$) and **8** (D_{4h}, $^1A_{1g}$). According to the recommended covalent atomic radii,[41] C–Al and Al–Al single bonds are around 2.0 and 2.5 Å, respectively. Thus **4** has typical C–Al single bonds, as anticipated. Those in LM **5** are beyond single bonds, suggesting delocalized C–Al bonding within the CAl_3 unit in addition to single bonds. Structures **6–8** have similar C–Al and Al–Al distances, except for a slight shrink upon addition of charges. Again, WBIs are smaller than the bond orders described above, due to the ionic nature of C–Al bonding (Fig. S4, ESI†).

To gain insight into bonding of the 16-electron quasi-ptC CBe_4Au_4 (**1**) cluster and C_{2v} CAl_4 (**5**), we optimized relevant C_{4v} (**9–11**) and T_d structures of isovalent CBe_4M_4 (M = K, H, Cl) clusters, as illustrated in Fig. S5 and S6 (ESI†). Note that **10** and **11** are LM structures only. Compared to CBe_4Au_4 (**1**), the C–Be distances in **9–11** (1.60–1.63 Å) virtually do not change. The Be–Be distances in **1** (2.18 Å) and **9** (2.21 Å) are also similar, whereas those in **11** (2.11 Å) and in particular **10** (1.93 Å) are markedly shortened. Likewise, atomic charges on the C center are similar for **1**, **9**, and **11** (−2.12, −2.32, and −2.28 $|e|$), as compared to a lower one for **10** (−1.56 $|e|$).

For T_d clusters, the C–Be distances are nearly identical for CBe_4M_4 (M = K, Au, H, Cl), amounting to 1.63–1.64 Å. Atomic charges on C decrease smoothly along the series, but the overall changes are moderate: −2.88, −2.64, −2.52, and −2.48 $|e|$. In contrast, charges on Be differ significantly along the series

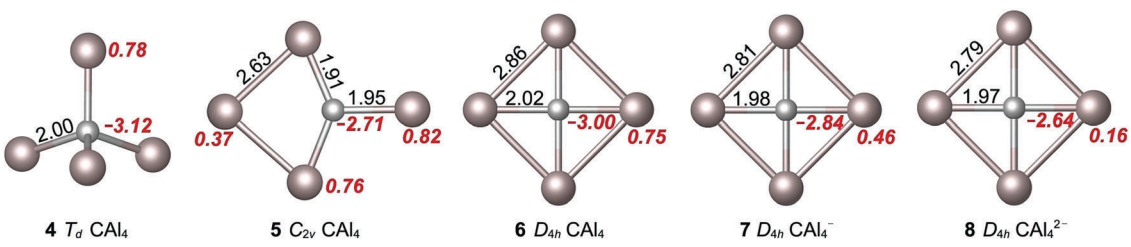

Fig. 2 Selected optimized structures of $CAl_4^{0/-/2-}$ clusters at the B3LYP/def2-TZVP level: GM for neutral (**4**, T_d, $^1A_1$); local-minimum (LM) for neutral (**5**, C_{2v}, $^1A_1$), 9.55 kcal mol^{-1} above GM at single-point CCSD(T); planar tetracoordinate carbon (ptC) neutral (**6**, D_{4h}, $^1A_1$) as a third-order saddle point, 15.30 kcal mol^{-1} above GM; GM for monoanion (**7**, D_{4h}, $^2B_{2g}$); and GM for dianion (**8**, D_{4h}, $^1A_{1g}$). Bond distances (in Å) and natural atomic charges (in $|e|$; red color) are shown.

(0.28, 0.84, 1.04, and 1.04 $|e|$, respectively), due to the distinct bonding of Be–K, Be–Au, Be–H, and Be–Cl. Following the above trend, charges on M are +0.44, −0.18, −0.41, and −0.42 $|e|$ along the series.

3.3. Molecular dynamics of $CBe_4Au_4^{0/-/2-}$ clusters

Thermodynamic and molecular dynamic stability of a ptC or quasi-ptC species benefits its potential synthesis in the gas phase. Born–Oppenheimer molecular dynamics (BOMD) simulations were performed for clusters **1–3** at the B3LYP/C,Be/6-31G(d)/Au/lanl2dz level, for 30 ps at room temperature (298 K). All species **1–3** maintain their structural integrity and ptC or quasi-ptC geometry during BOMD simulations (Fig. 3), which are robust against isomerization and decomposition. Major spikes in **1** and **2** are due to inversion vibration of C up and down the Be_4 plane, which is associated with their quasi-planar C_{4v} geometry, suggesting that the Be_4 ring is quite soft. The observation is in line with their low Be–Be bond order (0.20–0.23; Fig. S2, ESI†). The frequent occurrence of inversion spikes in **2** is consistent with its lower inversion barrier: 0.35 kcal mol^{-1} for **2** *versus* 2.54 kcal mol^{-1} for **1** at B3LYP/def2-TZVP.

4. Discussion

4.1. Robustness of the quasi-ptC CBe_4Au_4 cluster and its 16-electron counting

Our CK searches clearly show that, among neutral, monoanion, and dianion $CBe_4Au_4^{0/-/2-}$ clusters, the potential energy surface of CBe_4Au_4 is much simpler (Fig. S1, ESI†). Indeed, the quasi-ptC CBe_4Au_4 **1** (C_{4v}, $^1A_1$) cluster is well defined as GM, with an edge of

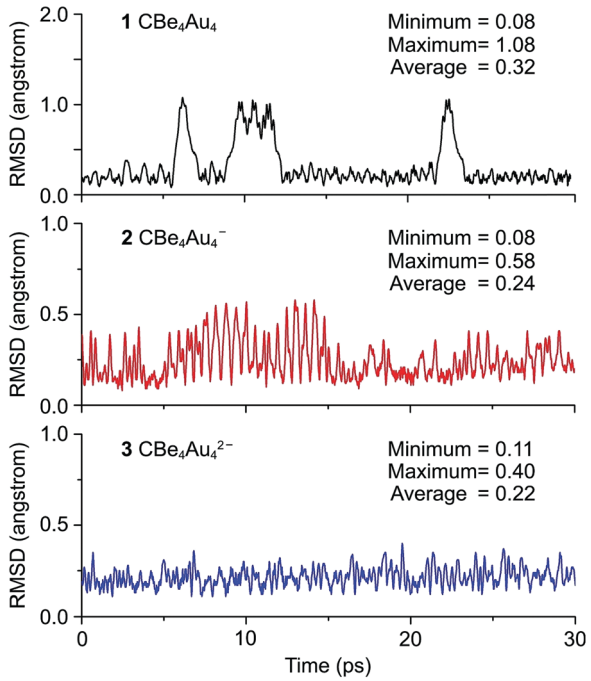

Fig. 3 Root-mean-square deviations (RMSD) of the ptC or quasi-ptC GM structures **1–3** of $CBe_4Au_4^{0/-/2-}$ clusters during Born–Oppenheimer molecular dynamics (BOMD) simulations at 298 K.

14.60 kcal mol^{-1} at CCSD(T). While the overall out-of-plane distortion of C gradually diminishes from 0.52, 0.38, to 0.00 Å in **1–3**, the energetics also decreases to 4.15 and 5.49 kcal mol^{-1} in **2** and **3**, respectively. It is thus fair to conclude that the CBe_4Au_4 (**1**) cluster is energetically robust.

In fact, CBe_4Au_4 (**1**) is the first ptC or quasi-ptC species with 16-electron counting, to our knowledge. It is electronically robust as well, despite the fact that a 16-electron system does not conform to the 18-electron "rule".[6–11,14–24] Based on the TD-B3LYP calculations, a simulated PES spectrum of the mono-anion quasi-ptC C_{4v} $CBe_4Au_4^-$ (**2**) cluster is generated (Fig. 4). The ground-state $^1A_1$ band has a rather low VDE of 1.57 eV, followed by a sizable energy gap of ~2.2 eV. Both numbers are indicative of electronic inertness of the CBe_4Au_4 (**1**) neutral species, which has a low EA value and a large HOMO–LUMO gap, justifying a stable 16-electron system. Quantitatively, the EA of CBe_4Au_4 (**1**) is calculated to be 1.54 at the B3LYP level and further refined to 1.28 eV at single-point CCSD(T). In contrast, the 18-electron CAl_4^{2-} (**8**) based $NaCAl_4^-$ cluster[9] has an experimental adiabatic detachment energy (ADE) of 2.02 eV and a small energy gap of 0.63 eV.

We shall now comment on the electron-counting "rule" of ptC and ppC complexes. Existing knowledge favors the 18-electron counting,[6–11,14–22] which contains four/five lone-pairs on ligands for ptC/ppC species, respectively. Complexes with other electron-counting are rare but still possible. For example, (i) ptC CLi_3E (E = As–Bi) and CLi_3E^+ (E = O–Po) were reported as 12-electron GM structures,[48] albeit with presumably only one lone-pair; (ii) ptC Si_2CH_2 was computed as LM with 14-electron;[49] (iii) ptC CB_4^+ as GM has 15 electrons;[50] (iv) ptC CAl_4^- and CAl_3E (E = Si, Ge) follow 17-electron counting;[8,10] (v) ptC C_5^{2-} has 22 electrons;[51] and (vi) phC CB_6^{2-} has 24-electron counting.[12] The above survey suggests that the 18-electron rule, which has been useful in the field of planar hypercoordinate carbons, should be viewed as a guide rather than a law. The present 16-electron quasi-ptC system offers yet a new exception for the "rule". As we will show below, it is not the number of electrons that dictates the ptC or quasi-ptC complexes, it is double (π and σ) aromaticity that underlies such species.

4.2. Chemical bonding in the quasi-ptC CBe_4Au_4 cluster

Why is 16-electron quasi-ptC CBe_4Au_4 (**1**) cluster stable? Bonding analyses provide the key insight. Fig. 5 depicts all CMOs of **1**, including the LUMO. Its eight occupied CMOs can be divided into three mutually orthogonal subsystems: (i) four CMOs that are largely Au s/d based (Fig. 5(b)), which can readily be transformed to four Be–Au–Be 3c-2e σ bonds on the periphery; (ii) a σ sextet (Fig. 5(d)) akin to the prototypical π sextet in benzene, which is globally delocalized with components from the C center, the inner Be_4 ring, and the peripheral Be_4Au_4 ring (Table S1, ESI†); (iii) a 2π delocalized subsystem being located primarily on the CBe_4 core (Fig. 5(c)). Adaptive natural density partitioning (AdNDP)[52] elegantly recovers the above picture; see Fig. 6.

In short, CMO and AdNDP bonding analyses suggest that 16-electron counting is ideal for quasi-ptC CBe_4Au_4 (**1**) species, which features 2π and 6σ double aromaticity in addition to four peripheral 3c-2e Be–Au–Be σ bonds. Indeed, for this ternary

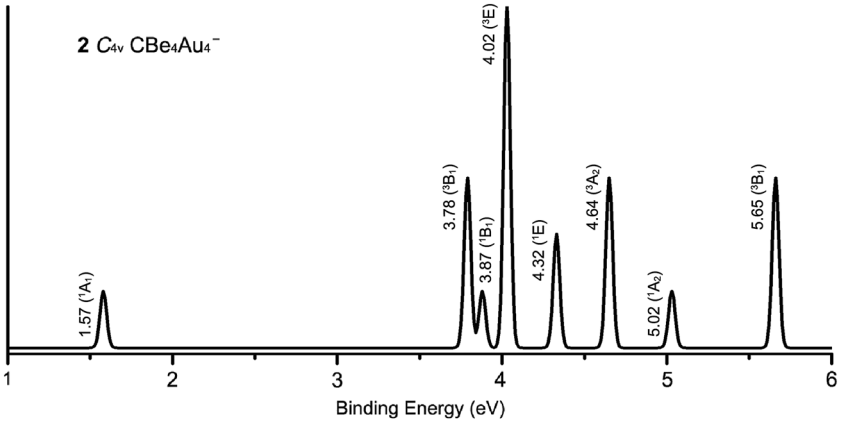

Fig. 4 Simulated photoelectron spectrum of the quasi-ptC C_{4v} $CBe_4Au_4^-$ (**2**) anion cluster, using the time-dependent B3LYP (TD-B3LYP) method. The simulation was done by fitting the distribution of calculated VDEs with unit-area Gaussian functions of 0.04 eV halfwidth.

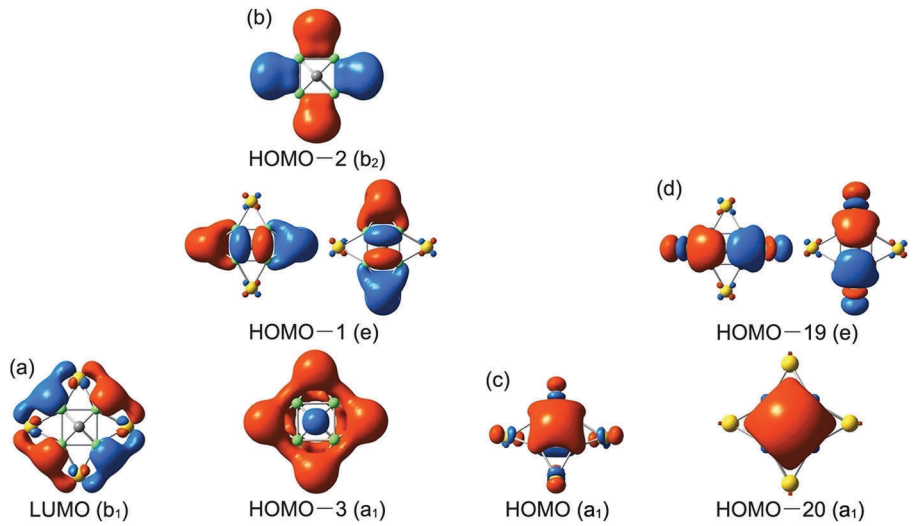

Fig. 5 Canonical molecular orbitals (CMOs) of the 16-electron quasi-ptC C_{4v} CBe_4Au_4 (**1**) cluster. (a) LUMO. (b) Four σ CMOs based on Be s/p and Au s/d atomic orbitals (AOs), which can be transformed into four Be–Au–Be three-center two-electron (3c-2e) σ bonds. (c) One π CMO located on the CBe_4 core. (d) Three radial σ CMOs, primarily located on the CBe_4 core. The delocalized (c) 2π and (d) 6σ subsystems render double aromaticity for the cluster.

system, the LUMO is dominated by four-center Be s/p interaction, which is formally antibonding between neighboring Be atoms (although it is weakly bonding as far as an eight-membered Be_4Au_4 ring is concerned). For such a system, 17- or 18-electron counting does not gain much extra bonding, thus further reinforcing the importance of 16-electron counting. Double aromaticity in **1** is independently confirmed *via* NICS calculations (Fig. S7, ESI†).[53] We believe that the concept of double (π and σ) aromaticity applies for all planar hypercoordinate carbons,[1,2] which explains why 18-electron counting is not necessarily a rule for such species (see Section 4.1). This understanding also opens the door for the rational design of 2D clusters with yet unknown electron-counting.

For comparison, the isovalent C_{2v} CAl_4 (**5**) cluster has a different bonding pattern (Fig. S8(a), ESI†). Its HOMO−3 is a global 2π bond, whereas HOMO−7 is a delocalized radial σ bond mainly on the tricoordinate CAl_3 unit. The HOMO−5/HOMO−2 combination recovers two C–Al σ bonds in the vertical direction. Likewise, the HOMO−6/HOMO−4 combination is responsible for a C–Al σ bond on the right side and a rough Al 2s lone-pair on the left. HOMO−1 is primarily a 3c-2e Al–Al–Al σ bond, orienting tangentially to the Al_3C ring. Lastly, the HOMO is approximated to an Al 2s lone-pair at the right end. Thus C_{2v} CAl_4 (**5**) is also doubly delocalized, albeit with 2π and 2σ electrons only. The Al_3C ring in **5** features 2π aromaticity and weaker 2σ aromaticity, because the electron cloud of the latter leans to the right. The bonding pattern of T_d CAl_4 (**4**) is much simpler, with four C–Al σ bonds and four Al 2s lone-pairs (Fig. S8(b), ESI†).

4.3. Competition between quasi-ptC and thC isomers in CBe_4M_4 (M = K, Au, H, Cl)

To shed further light on the chemical bonding in ptC or quasi-ptC clusters and the competition between ptC and thC isomers, we examine the energetics of a series of 16-electron CBe_4M_4 (M = K, Au, H, Cl) clusters, that is, **1** and **9–11**, in which M covers a diversity of elements from alkali metal, coinage metal, hydrogen,

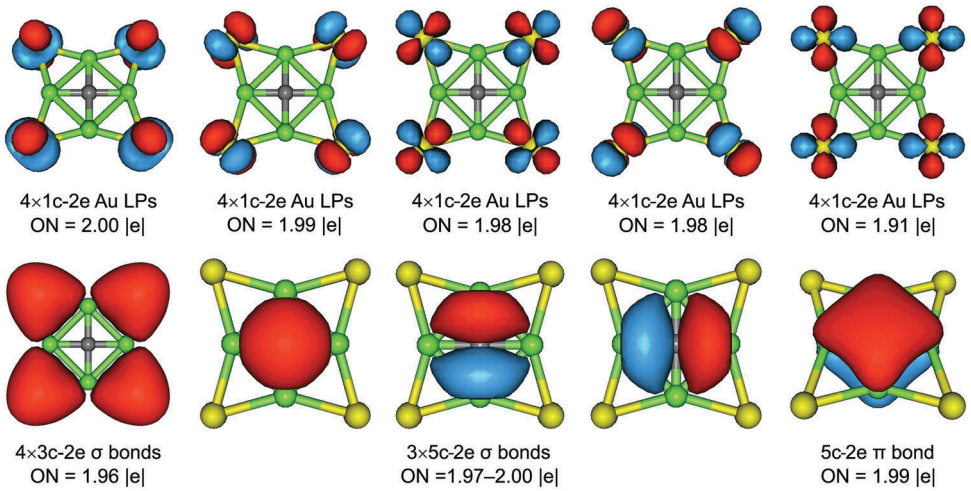

Fig. 6 Bonding pattern for the 16-electron quasi-ptC cluster C_{4v} CBe_4Au_4 (**1**) as revealed from adaptive natural density partitioning (AdNDP). LP stands for a lone pair. Occupation numbers (ONs) are indicated.

to halogen. Note that in CBe_4Cl_4 (**11**), each Cl ligand maintains three lone-pairs and can be viewed as valence one. Thus **11** is effectively a 16-electron system. Optimized structures, NBO charges, and WBIs of CBe_4M_4 (M = K, Au, H, Cl) are presented in Fig. S5 and S6 (ESI†). All thC species assume T_d symmetry. For quasi-ptC C_{4v} species, the out-of-plane distortion of M spans a range of 0.31, 0.52, 0.88, and 0.66 Å for M = K–Cl, with CBe_4H_4 (**10**) having the greatest pyramidal distortion.

Relative energy (ΔE) between quasi-ptC and thC isomers of CBe_4M_4 depends sensitively on M, as illustrated in Fig. 7 for single-point CCSD(T) data. By definition, a negative ΔE means that a quasi-ptC isomer is more stable and *vice versa*. Thus, quasi-ptC is most favored for CBe_4Au_4 (by 14.82 kcal mol^{-1}), whereas CBe_4H_4 leans to thC by a large margin (43.04 kcal mol^{-1}). This observation is remarkable, in particular, considering the fact of Au/H isolobal analogy in mixed clusters.[45–47] To rationalize the trend, we mention just a few points. First, C–Be–Au bonding in CBe_4Au_4 (**1**) appears to be most delocalized as revealed from the orbital component analysis of the HOMO with global contributions from C/Be_4/Au_4 (Table S2, ESI†), and the geometric

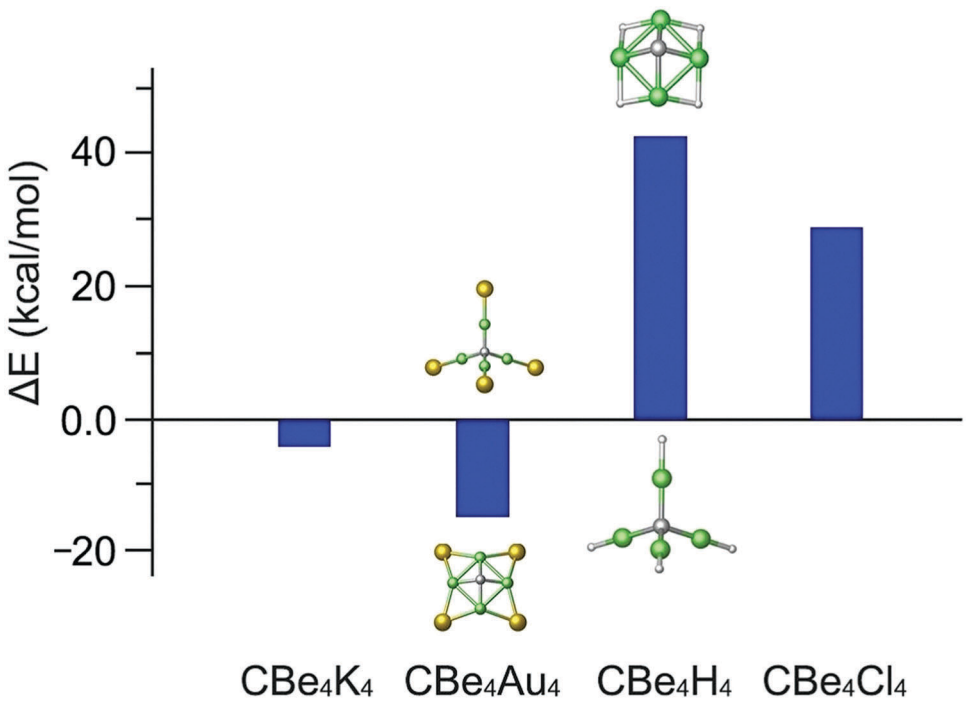

Fig. 7 Relative energy (ΔE) of quasi-ptC *versus* thC structures of the CBe_4M_4 (M = K, Au, H, Cl) series at the single-point CCSD(T) level, with zero-point energy (ZPE) corrections at B3LYP/def2-TZVP. The thC species is used as reference and negative ΔE indicates that the quasi-ptC structure is more stable. The quasi-ptC CBe_4Au_4 (**1**) and thC CBe_4H_4 species show remarkable stability.

size of this quasi-ptC cluster is among the largest (Fig. S5, ESI†). Both factors stabilize **1** as a doubly aromatic system. In contrast, the HOMO of **9** is confined within CBe_4, as is that of **10**. Second, the maximum of out-of-plane distortion in **10** (0.88 Å) is a con for π/σ delocalization and thus destabilizes it. This distortion is due to the small size of H atom, which makes the shortest Be–Be distance in the Be_4 ring (1.93 Å; Fig. S5, ESI†) and pushes the C center out significantly. Third, the T_d isomer gains stability *via* C–Be–M σ conjugation, as exemplified by the HOMO. In particular, T_d CBe_4H_4 shows a maximum of σ conjugation, which is completely delocalized on C/Be/H (Table S3, ESI†), thus explaining why quasi-ptC CBe_4H_4 (**10**) has the least relative stability (Fig. 7). Lastly, we comment that the instability of isomer **5** of CAl_4 (relative to **4**) is likely associated with substantial Coulomb repulsion. Indeed, the C center in **5** carries the largest amount of negative charges among all quasi-planar species (Fig. S5, ESI†). A T_d configuration such as **4** can effectively reduce the Coulomb repulsion. By putting in extra charges, atomic charges on Al sites decrease steadily in **7** and **8**, making the ptC isomer competitive (Fig. 2).

5. Conclusions

We have computationally designed a ternary quasi-planar tetracoordinate carbon (quasi-ptC) cluster, C_{4v} CBe_4Au_4. It is clearly the global minimum of the system *via* computer structural searches. With 16-electron counting, the quasi-ptC cluster does not follow the 18-electron rule, which dominates planar hypercoordinate carbon complexes. Chemical bonding analyses suggest that CBe_4Au_4 has four three-center two-electron (3c-2e) Be–Au–Be σ bonds, being further stabilized by 2π and 6σ double aromaticity, which conform to the $(4n + 2)$ Hückel rule. This bonding pattern helps rationalize the 16-electron counting as an ideal choice for the system. The competition between quasi-ptC and tetrahedral carbon (thC) isomers in the isovalent CBe_4M_4 (M = K, Au, H, Cl) series sheds light on key factors that govern the ptC or quasi-ptC clusters, such as the extent of electron delocalization, ring size surrounding the C center, and σ conjugation in the rivaling thC cluster.

Conflicts of interest

There are no conflicts to declare.

Acknowledgements

This work was supported by the National Natural Science Foundation of China (21573138), the Scientific and Technological Innovation Programs of Higher Education Institutions in Shanxi (2017170), and the Sanjin Scholar Distinguished Professors Program.

References

1 L. M. Yang, E. Ganz, Z. F. Chen, Z. X. Wang and P. v. R. Schleyer, *Angew. Chem., Int. Ed.*, 2015, **54**, 9468.
2 R. Keese, *Chem. Rev.*, 2006, **106**, 4787.
3 H. J. Monkhorst, *Chem. Commun.*, 1968, 1111.
4 R. Hoffmann, R. W. Alder and C. F. Wilcox, *J. Am. Chem. Soc.*, 1970, **92**, 4992.
5 J. B. Collins, J. D. Dill, E. D. Jemmis, Y. Apeloig, P. v. R. Schleyer, R. Seeger and J. A. Pople, *J. Am. Chem. Soc.*, 1976, **98**, 5419.
6 P. v. R. Schleyer and A. I. Boldyrev, *J. Chem. Soc., Chem. Commun.*, 1991, 1536.
7 A. I. Boldyrev and J. Simons, *J. Am. Chem. Soc.*, 1998, **120**, 7967.
8 X. Li, L. S. Wang, A. I. Boldyrev and J. Simons, *J. Am. Chem. Soc.*, 1999, **121**, 6033.
9 X. Li, H. F. Zhang, L. S. Wang, G. D. Geske and A. I. Boldyrev, *Angew. Chem., Int. Ed.*, 2000, **39**, 3630.
10 L. S. Wang, A. I. Boldyrev, X. Li and J. Simons, *J. Am. Chem. Soc.*, 2000, **122**, 7681.
11 Y. Pei, W. An, K. Ito, P. v. R. Schleyer and X. C. Zeng, *J. Am. Chem. Soc.*, 2008, **130**, 10394.
12 Z. X. Wang and P. v. R. Schleyer, *Science*, 2001, **292**, 2465.
13 A. D. Zdetsis, *J. Chem. Phys.*, 2011, **134**, 094312.
14 J. O. C. Jimenez-Halla, Y. B. Wu, Z. X. Wang, R. Islas, T. Heine and G. Merino, *Chem. Commun.*, 2010, **46**, 8776.
15 Y. B. Wu, Y. Duan, H. G. Lu and S. D. Li, *J. Phys. Chem. A*, 2012, **116**, 3290.
16 A. C. Castro, G. Martínez-Guajardo, T. Johnson, J. M. Ugalde, Y. B. Wu, J. M. Mercero, T. Heine, K. J. Donald and G. Merino, *Phys. Chem. Chem. Phys.*, 2012, **14**, 14764.
17 R. Grande-Aztatzi, J. L. Cabellos, R. Islas, I. Infante, J. M. Mercero, A. Restrepo and G. Merino, *Phys. Chem. Chem. Phys.*, 2015, **17**, 4620.
18 J. C. Guo, G. M. Ren, C. Q. Miao, W. J. Tian, Y. B. Wu and X. Wang, *J. Phys. Chem. A*, 2015, **119**, 13101.
19 A. C. Castro, M. Audiffred, J. M. Mercero, J. M. Ugalde, M. A. Méndez-Rojas and G. Merino, *Chem. Phys. Lett.*, 2012, **519–520**, 29.
20 Z. H. Cui, Y. H. Ding, J. L. Cabellos, E. Osorio, R. Islas, A. Restrepo and G. Merino, *Phys. Chem. Chem. Phys.*, 2015, **17**, 8769.
21 J. Xu, X. X. Zhang, S. Yu, Y. H. Ding and K. H. Bowen, *J. Phys. Chem. Lett.*, 2017, **8**, 2263.
22 Z. H. Cui, V. Vassilev-Galindo, J. L. Cabellos, E. Osorio, M. Orozco, S. Pan, Y. H. Ding and G. Merino, *Chem. Commun.*, 2017, **53**, 138.
23 E. Janssens, H. Tanaka, S. Neukermans, R. E. Silverans and P. Lievens, *New J. Phys.*, 2003, **5**, 46.
24 W. D. Knight, K. Clemenger, W. A. de Heer, W. A. Saunders, M. Y. Chou and M. L. Cohen, *Phys. Rev. Lett.*, 1984, **52**, 2141.
25 A. P. Sergeeva, B. B. Averkiev, H. J. Zhai, A. I. Boldyrev and L. S. Wang, *J. Chem. Phys.*, 2011, **134**, 224304.
26 M. Saunders, *J. Comput. Chem.*, 2004, **25**, 621.
27 P. P. Bera, K. W. Sattelmeyer, M. Saunders, H. F. Schaefer III and P. v. R. Schleyer, *J. Phys. Chem. A*, 2006, **110**, 4287.
28 P. J. Hay and W. R. Wadt, *J. Chem. Phys.*, 1985, **82**, 270.
29 P. J. Hay and W. R. Wadt, *J. Chem. Phys.*, 1985, **82**, 299.
30 F. Weigend and R. Ahlrichs, *Phys. Chem. Chem. Phys.*, 2005, **7**, 3297.
31 J. A. Pople, M. Head-Gordon and K. Raghavachari, *J. Chem. Phys.*, 1987, **87**, 5968.

32 G. E. Scuseria, C. L. Janssen and H. F. Schaefer III, *J. Chem. Phys.*, 1988, **89**, 7382.
33 G. E. Scuseria and H. F. Schaefer III, *J. Chem. Phys.*, 1989, **90**, 3700.
34 A. E. Reed, L. A. Curtiss and F. Weinhold, *Chem. Rev.*, 1988, **88**, 899.
35 P. v. R. Schleyer, C. Maerker, A. Dransfeld, H. J. Jiao and N. J. R. v. E. Hommes, *J. Am. Chem. Soc.*, 1996, **118**, 6317.
36 M. E. Casida, C. Jamorski, K. C. Casida and D. R. Salahub, *J. Chem. Phys.*, 1998, **108**, 4439.
37 R. Bauernschmitt and R. Ahlrichs, *Chem. Phys. Lett.*, 1996, **256**, 454.
38 M. J. Frisch, G. W. Trucks, H. B. Schlegel, G. E. Scuseria, M. A. Robb, J. R. Cheeseman, G. Scalmani, V. Barone, B. Mennucci, G. A. Petersson, H. Nakatsuji, M. Caricato, X. Li, H. P. Hratchian, A. F. Izmaylov, J. Bloino, G. Zheng, J. L. Sonnenberg, M. Hada, M. Ehara, K. Toyota, R. Fukuda, J. Hasegawa, M. Ishida, T. Nakajima, Y. Honda, O. Kitao, H. Nakai, T. Vreven, J. A. Montgomery, J. E. Peralta, F. Ogliaro, M. Bearpark, J. J. Heyd, E. Brothers, K. N. Kudin, V. N. Staroverov, R. Kobayashi, J. Normand, K. Raghavachari, A. Rendell, J. C. Burant, S. S. Iyengar, J. Tomasi, M. Cossi, N. Rega, J. M. Millam, M. Klene, J. E. Knox, J. B. Cross, V. Bakken, C. Adamo, J. Jaramillo, R. Gomperts, R. E. Stratmann, O. Yazyev, A. J. Austin, R. Cammi, C. Pomelli, J. W. Ochterski, R. L. Martin, K. Morokuma, V. G. Zakrzewski, G. A. Voth, P. Salvador, J. J. Dannenberg, S. Dapprich, A. D. Daniels, O. Farkas, J. B. Foresman, J. V. Ortiz, J. Cioslowski and D. J. Fox, *GAUSSIAN 09, Revision D.01*, Gaussian, Inc., Wallingford, CT, 2009.
39 C. Y. Legault, *CYLview, 1.0b*, Université de Sherbrooke, 2009, http://www.cylview.org.
40 R. Dennington, T. Keith and J. Millam, *GaussView, Version 5*, Semichem, Inc., Shawnee Mission, KS, 2009.
41 P. Pyykkö, *J. Phys. Chem. A*, 2015, **119**, 2326.
42 A. Kalemos, *J. Chem. Phys.*, 2016, **145**, 214302.
43 I. O. Antonov, B. J. Barker, V. E. Bondybey and M. C. Heaven, *J. Chem. Phys.*, 2010, **133**, 074309.
44 Z. X. Wang, C. G. Zhang, Z. F. Chen and P. v. R. Schleyer, *Inorg. Chem.*, 2008, **47**, 1332.
45 B. Kiran, X. Li, H. J. Zhai, L. F. Cui and L. S. Wang, *Angew. Chem., Int. Ed.*, 2004, **43**, 2125.
46 H. J. Zhai, L. S. Wang, D. Y. Zubarev and A. I. Boldyrev, *J. Phys. Chem. A*, 2006, **110**, 1689.
47 H. J. Zhai, C. Q. Miao, S. D. Li and L. S. Wang, *J. Phys. Chem. A*, 2010, **114**, 12155.
48 J. Y. Guo, H. Y. Chai, Q. Duan, J. M. Qin, X. D. Shen, D. Y. Jiang, J. H. Hou, B. Yan, Z. R. Li, F. L. Gu and Q. S. Li, *Phys. Chem. Chem. Phys.*, 2016, **18**, 4589.
49 S. Vogt-Geisse, J. I-Chia Wu, P. v. R. Schleyer and H. F. Schaefer III, *J. Mol. Model.*, 2015, **21**, 217.
50 Z. H. Cui, M. Contreras, Y. H. Ding and G. Merino, *J. Am. Chem. Soc.*, 2011, **133**, 13228.
51 G. Merino, M. A. Mendez-Rojas and A. Vela, *J. Am. Chem. Soc.*, 2003, **125**, 6026.
52 D. Y. Zubarev and A. I. Boldyrev, *Phys. Chem. Chem. Phys.*, 2008, **10**, 5207.
53 Note that ptC (or quasi-ptC) clusters **2** and **3**, with 17- and 18-electron counting, respectively, are also doubly aromatic with 2π and 6σ electrons.

